

Wind-Tunnel Investigation of a B-52 Model Flutter Suppression System

L. T. Redd* and J. Gilman Jr.†

NASA Langley Research Center, Hampton, Va.

and

D. E. Cooley‡

U.S. Air Force Flight Dynamics Laboratory, Wright-Patterson Air Force Base, Ohio

and

F. D. Severt§

Boeing Company, Wichita, Kansas

Flutter modeling techniques have been successfully extended to the difficult case of the active suppression of flutter. This has been demonstrated in a joint USAF/NASA/Boeing (Wichita Div.) study. The demonstration was conducted in the NASA Langley transonic dynamics tunnel using a 1/30-scale, elastic, dynamic model of a Boeing B-52 Control Configured Vehicle (CCV). The results from the study show that with the flutter suppression system operating there is a substantial increase in the damping associated with the critical flutter mode. The results also show good correlation between the damping characteristics of the model and airplane.

Introduction

THERE is considerable interest in the application of active control technology toward the reduction of aircraft aeroelastic responses. Use of active control systems to provide fatigue reduction, gust alleviation, maneuver load control, augmented stability, and flutter suppression offers potential for significant improvements in aircraft performance and considerable weight savings. The application of active controls to reduce airplane dynamic response has already been demonstrated during the past decade on the XB-70 and B-52 airplanes.^{1,2} The success of the latter application has led to a joint USAF/Boeing (Wichita Div.) program to further investigate the use of active control technology to provide more efficient aircraft in the future. This effort has resulted in a program to demonstrate advanced active control concepts in flight tests using B-52 Control Configured Vehicles (CCV) research aircraft.^{3,4}

In conjunction with the USAF/Boeing CCV program, a joint NASA/USAF/Boeing (Wichita Div.) wind-tunnel research program was initiated using a 1/30-sized dynamically scaled aeroelastic model of the CCV research aircraft.^{5,6} The model was equipped with active control systems to simulate the flutter suppression, ride control, and maneuver load control systems of the research airplane. The objective of the wind-tunnel research program was to obtain model test results for comparison with those from CCV flight tests and from analysis to demonstrate that airplane active control systems can be successfully simulated with wind-tunnel models and that models can be used to validate analytical results. Considerable cost savings and increased safety can be realized if wind-tunnel model tests can be used to develop, evaluate, and proof-test candidate full-scale aircraft active control systems.

The present paper is concerned with the flutter-suppression portion of the B-52 CCV model wind-tunnel study. Essential details of the model and flutter mode control (FMC) system are presented and test procedures are explained. The paper includes a description of data reduction procedures and comparisons of model results with analytical predictions and flight-test results.

Model Description

A photograph of the model installed in the Langley transonic dynamics wind tunnel is shown in Fig. 1. The 1/30-size model had a wing span of 188 cm (6.16 ft) and weighed 26 kgm (57.4 lb). The model was originally designed for low-speed gust response studies and was thus scaled on the basis of equal Froude number and mass ratio to match the B-52E airplane.^{7,8} The stiffness and mass distributions were also scaled to match the B-52E airplane. The model stiffness was provided by aluminum alloy fuselage and wing spars which were covered with flexible segmented pod fairings (Fig. 1) to provide the correct aerodynamic contour.

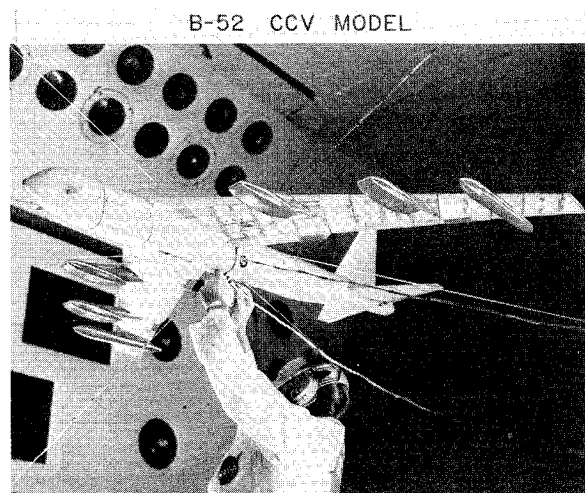


Fig. 1 B-52 CCV model mounted in the Langley transonic dynamics tunnel.

Presented as Paper 74-401 at the AIAA/ASME/SAE 15th Structures, Structural Dynamics and Materials Conference, Las Vegas, Nev., April 17-19, 1974; submitted April 25, 1974; revision received July 12, 1974.

Index categories: Aeroelasticity and Hydroelasticity; Aircraft Handling, Stability, and Control; Aircraft Vibration.

*Aero-Space Engineer, Aeroelasticity Branch, Structures and Dynamics Division.

†Aero-Space Engineer, Retired.

‡Group Leader, Vehicle Dynamics Division. Member AIAA.

§Specialist Engineer, Flight Controls Development.

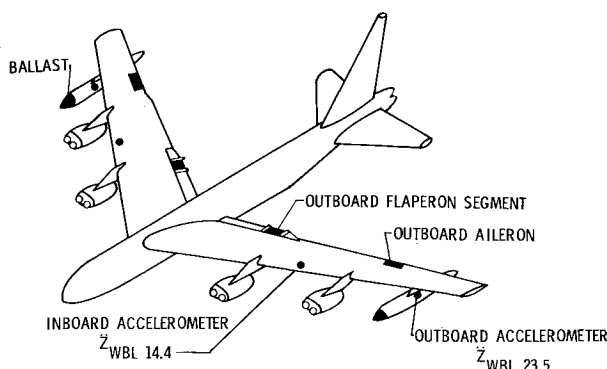


Fig. 2 B-52 model control surfaces and sensors used for flutter suppression.

Flutter Configuration

Since the B-52E airplane is normally flutter free throughout the operational flight envelope, it was necessary to make modifications to the airplane for the CCV flutter tests. These modifications consisted of adding 907 kg (2000 lb) of ballast to the nose of the empty wing-tip fuel tanks and redistributing the load in the remaining fuel tanks to give the proper airplane c.g. and total gross weight of 170,000 kg (375,000 lb). The original B-52E model wing-tip tanks and model mass distribution were also modified according to the equal Froude number and mass ratio scaling relationships to simulate the CCV airplane flutter configuration. In addition, the model was tested in Freon gas at a density of 2.574 kg/m³ (0.00499 slug/ft³) to simulate the airplane flutter test altitude of 6401 m (21,000 ft). Because the elastic modes of the original model outboard nacelle struts did not properly simulate those of the CCV airplane and analytical studies indicated the flutter speed was very sensitive to the nacelle strut stiffness,⁹ new outboard struts were fabricated.

Flutter Mode Control System

The primary objective of the active control flutter-suppression study is to develop a flutter mode control (FMC) system which will increase the airplane flutter placard velocity by at least 30%.¹⁰ The design of the FMC system used to obtain this objective is based on the results of previous experience and analysis of the B-52 airplane. These results indicate that the aerodynamic forces on the wing are stabilizing over the entire flutter oscillation cycle when the incremental lift generated by the control surfaces lags the wing displacement by 90°. Thus the FMC system operates as a closed-loop-control system which provides the required phase lag between wing lift and displacement at the flutter frequency. Signals from accelerometer pickups on the wing are modified by appropriate shaping filters and are then fed back as command signals to drive control surfaces on the wing. The positions of the wing accelerometers and the aileron and flaperon control surfaces used in model and airplane flutter suppression system are shown in Fig. 2. In terms of the full-scale airplane dimensions, the wing accelerators are located at wing buttock line (WBL) 23.5 m (925 in.) and WBL 14.4 m (565 in.) on both the left and right wings. The model outboard accelerometers $\ddot{Z}_{WBL\ 23.5}$ are located in the external tip tanks because of the limited volume available in the wing airfoil at WBL 23.5.

A functional block diagram of the model FMC system is shown in Fig. 3. The system senses vertical accelerations at WBL 23.5 and WBL 14.4 for the left and right wings independently. The acceleration signals at WBL 23.5 from each wing are summed to filter out unsymmetrical motions, multiplied by a factor of 0.5, and the resulting sig-

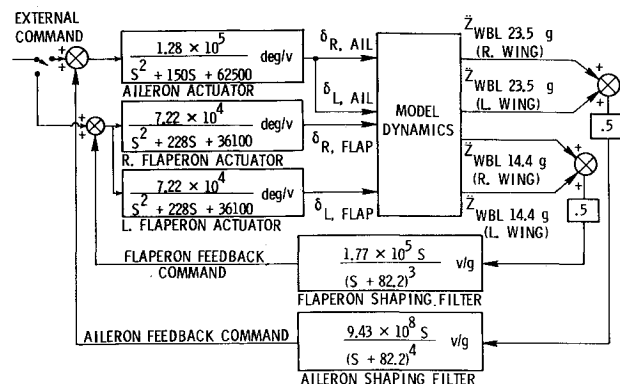


Fig. 3 Model flutter mode control system functional block diagram.

nal is passed to the aileron shaping filter. A second set of acceleration signals at WBL 14.4 are similarly summed and passed to the flaperon shaping filter. The shaping filter transfer functions shown in Fig. 3 are identical to those for the airplane except the model filter cutoff frequencies are scaled by the model scale factor 5.48. The signals from the shaping filters are passed to a second set of summing junctions where external command signals to the aileron or flaperon control surfaces can be added. The external command signals are used only to drive the control surfaces when the FMC system is either off or on. Note that the right and left flaperon control surfaces are driven from separate actuator systems (Fig. 3), but the two ailerons have the same actuator.

The outboard aileron and flaperon control loops shown in Fig. 3 can operate independently or collectively, and each provides the required increase in flutter mode damping. Thus, there is a complete redundancy in the FMC system.

The control surface actuator mechanism in the model used an electromechanical drive system, whereas an electrohydraulic actuator system was used in the airplane. Because different actuator systems were used in the model and airplane, the actuator transfer functions for the two FMC systems are not identical; however, the dynamic characteristics of the two systems were similar for the range of frequencies of interest. Thus the actuator transfer functions indicated in Fig. 3 only apply to the model. All other components of the FMC system for the model and airplane are equivalent. Although the analysis included

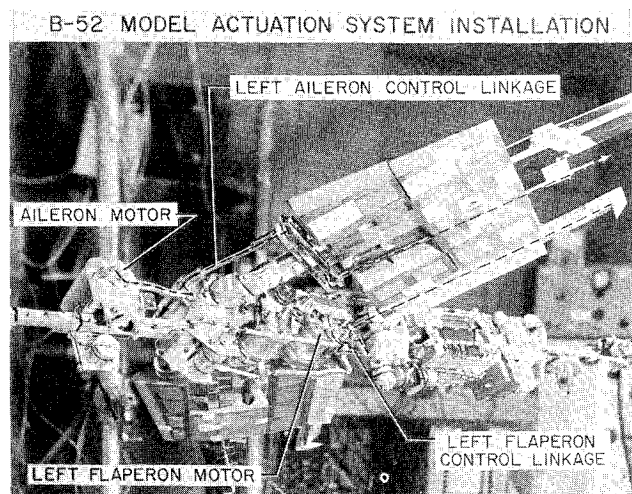


Fig. 4 B-52 model flaperon and outboard aileron actuation system installations (bottom view).

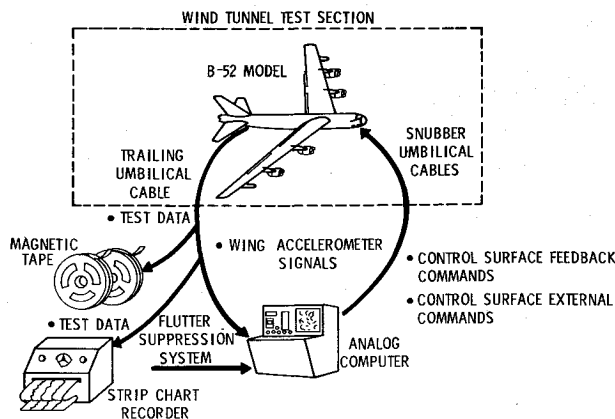


Fig. 5 Schematic of flutter mode control system test setup.

the differences in actuator transfer functions, the analytical results showed that the model and airplane FMC systems had essentially the same flutter suppression characteristics.¹⁰

The electromechanical actuator system for the model consisted of separate d.c. torque motors mounted within the fuselage to drive the ailerons and left and right flaperons. Torque from the motors was transmitted through crank-pushrod linkages and shafting to the control surfaces as shown in Fig. 4. The control linkages and shafting were designed to be isolated from the model structure so that they would not change the stiffness characteristics of the fuselage or wing. A more detailed description of the actuator system is given in Ref. 5.

Wind-Tunnel Tests

The primary objectives of the wind-tunnel tests were to establish the open-loop (i.e., FMC off) flutter velocity for the model, to demonstrate the effectiveness of the FMC system, and to obtain data for correlation with model analysis and airplane test results. The model test data obtained consisted of both steady-state and transient responses. The outboard aileron, flaperon, elevator, and horizontal canard control surfaces (Fig. 1) were used as model forcing functions. Response data were also obtained from aerodynamic inputs due to tunnel turbulence. From these various response measurements, the damping characteristics of the model were obtained.

Model Installation

The model was installed in the tunnel test section on a modified version of the two-cable mount system described in Ref. 11. This system provides for free-flight simulation with a minimum of restraint. The cable mount system also includes four snubber cables which are used for emergency restraint and are normally slack during tunnel testing.

FMC System Mechanization

A schematic of the power and data flow for the flutter suppression system used in the model test is shown in Fig. 5. The signals from the wing accelerometers were carried from the model to an analog computer through a trailing umbilical cable which came out of the model fuselage and aft to the tunnel sting. The shaping filter transfer functions were mechanized on an analog computer and the resulting feedback commands were routed to the actuators in the model through umbilical lines attached to the four snubber cables. The external command signals for model excitation were added to the FMC system through the analog computer. Signals from onboard model sensors

including the wing accelerometers were carried through the trailing umbilical cable to magnetic tape and strip chart recorders.

Response Measurements

Several techniques were used for determining model response characteristics during the wind-on testing. The most useful technique involved measuring the forced response of the model to a sinusoidal frequency sweep input generated by one of the model control surfaces. This frequency sweep technique used an analog signal analyzer which produced the in-phase and out-of-phase components of the wing accelerometer output relative to a control surface input. Sample results using this technique to measure the ratio of the right wing accelerations $\ddot{Z}_{WBL 23.5}$ to aileron command displacements $\delta_{ail. com.}$ are shown as functions of frequency in Fig. 6. The curves in the upper portion of the figure represent the frequency response of the basic model (i.e., FMC system off) and the lower curves show the response with the FMC control loop closed (i.e., FMC system on). The damping of the modes can be estimated from the in-phase component frequencies labeled f_A and f_B . For an equivalent single-degree-of-freedom system, these are the frequencies at approximately the half-power points, and the damping \tilde{g} can be expressed in terms of these frequencies:¹²

$$\tilde{g} = [(f_B/f_A)^2 - 1] / [(f_B/f_A)^2 + 1]$$

Although the preceding equation was derived for a single-degree-of-freedom system, the equation can be used with the present multidegree system to obtain good estimates of damping for the flutter mode provided the relative frequency and damping of the other modes do not appreciably affect the flutter mode. As can be seen in Fig. 6, the damping with the FMC system on is approximately four times greater than the damping with the system off. The velocity V shown in the title of this figure and in all succeeding figures is given in terms of full-scale airplane equivalent airspeeds.

A second technique used to measure model damping characteristics was based on the "Randomdec" method described in Ref. 13. This technique was used primarily to obtain the damped sinusoidal response of the model flutter mode for cases where the only excitation inputs were due to tunnel turbulence. This was accomplished by pass-

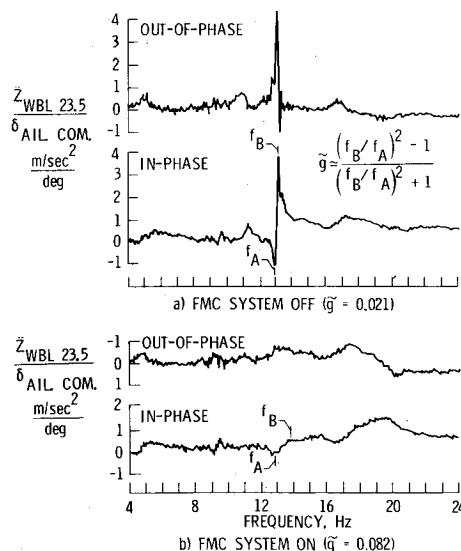


Fig. 6 Measured frequency response of the B-52 model to aileron excitation ($\delta_{ail. com.} = \pm 2^\circ$, $V = 237$ m/sec).

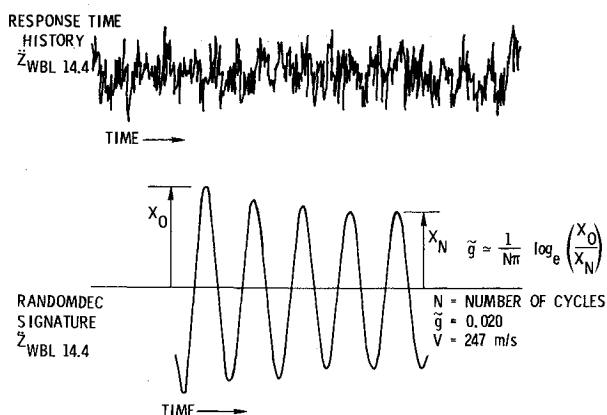


Fig. 7 Wing response at WBL 14.4 as measured with Randomdec technique.

ing the wing acceleration signals through ensemble averaging circuitry to obtain a decay trace from the random response. Since the model was a multidegree system, it was also necessary to pass the acceleration signals through a band-pass filter to isolate the flutter mode. Figure 7 shows a typical segment of a response time history trace for the right wing accelerometer $\dot{Z}_{WBL 14.4}$ signal and the corresponding Randomdec signature of the response. The damping was obtained from the logarithmic decrement of the Randomdec signature as shown in the figure. The Randomdec technique worked best as the flutter mode damping approached zero and was especially useful when conditions were approached where it was dangerous to apply external excitation. The damping estimates obtained from the Randomdec and frequency sweep techniques agreed very well as the damping of the flutter mode approached zero.

Additional techniques used to measure damping data included use of wing acceleration transient responses. One method involved exciting the wing with an outboard aileron sinusoidal command and then suddenly removing the command to give a transient response. A second method involved exciting the model with a one-cycle sine wave pulse from the elevator control surface to give the transient response. It was difficult to estimate a reliable flutter mode damping value from either of these methods due to the relatively large amount of wing accelerometer responses caused by tunnel turbulence.

Evaluation of Test Results

The most useful results obtained in the wind-tunnel test are contained in the forced response data generated by the sinusoidal frequency sweep technique. The particular forced response data of most significance are the results which relate the right outboard accelerometer $\dot{Z}_{WBL 23.5}$ response to the aileron command input. These results are used in this paper for correlation with model analytical data and airplane test results. The correlations are presented in the form of damping versus airplane equivalent airspeed in Figs. 8 and 9.

Comparison of Model Test and Analytical Data

A comparison of the measured and calculated damping characteristics of the model is shown in Fig. 8. The calculated damping values shown were obtained from the characteristic roots of the equations of motion. The equations of motion were derived using compressible, doublet lattice theory for the aerodynamic loading and lumped parameter idealization for the elastic and inertia characteristics of the model.⁹ The flutter analyses were performed for the lowest 24 symmetric and antisymmetric vibration modes

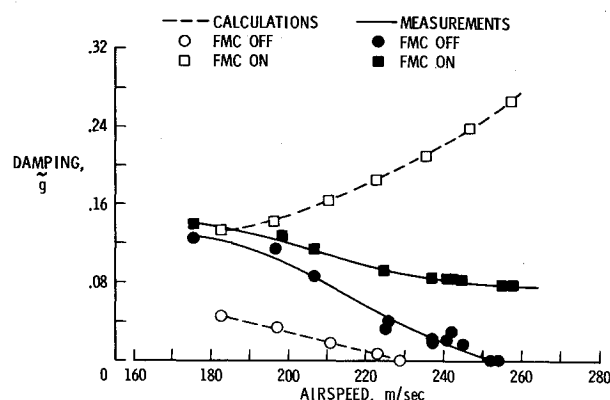


Fig. 8 Comparison of measured and calculated damping characteristics of the flutter mode for the B-52 model.

for the model supported on the two-cable mount system and in the free-free condition. The analytical damping values shown in Fig. 8 are for the flutter mode (i.e., the sixth symmetric mode) with the model supported on the two-cable mount system.

The measured data presented in Fig. 8 show the open-loop flutter point to be about 253 m/sec which is about 10% higher than the 229 m/sec flutter velocity predicted analytically. Part of this difference may be associated with the fact that the measured windoff structural damping ($\tilde{g} = 0.015$) for the flutter mode of the model was higher than the damping ($\tilde{g} = 0.005$) used in the flutter analysis.⁹ The difference between the model measured and calculated flutter speeds is about the same as that obtained between the measured and calculated flutter speeds of the airplane, the difference in the latter case being 8.3%. Thus, there is a consistency between the model and airplane analyses since the analysis in both cases predicted a lower flutter speed than was found experimentally.

Both the experimental and calculated data shown in Fig. 8 indicate that with the FMC system operating there is a substantial increase in damping near the open-loop flutter point. The measured damping data for the FMC system on condition show the system to be less effective than analytically predicted. Part of the difference may be due to the fact that the model had excessive hysteresis in the outboard aileron actuator system. The model control surface effectiveness is also believed to be less than assumed in the analysis.

The maximum velocity tested with the FMC system operating was 264 m/sec, but no damping values were measured above 258 m/sec. The maximum velocity is 11

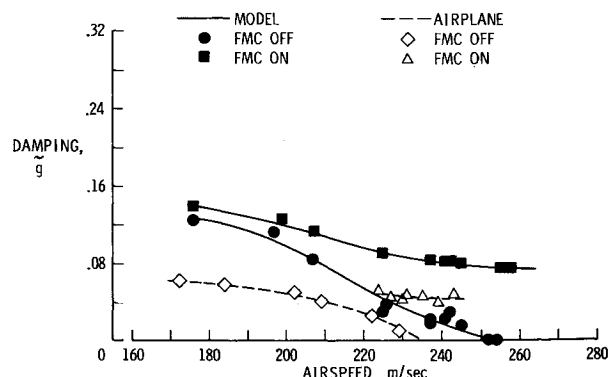


Fig. 9 Comparison of model and airplane damping characteristics of the flutter mode for the B-52 CCV airplane.

m/sec or 4.3% above the open-loop flutter velocity which exceeds an objective of the airplane flight tests (i.e., to demonstrate the airplane FMC system up to 6.5 m/sec (10 KCAS) above the open-loop flutter speed).

Comparison of Model and Airplane Data

A comparison of the measured model and airplane damping characteristics is shown in Fig. 9. The airplane damping values shown were obtained from transient response records. The data show that the model open-loop flutter speed is 7.9% higher than the airplane flutter speed of 235 m/sec. Some of the reasons for the differences in the two flutter speeds are attributed to minor variations in model mass and stiffness properties from the required scaled values, and to cable mount effects on the rigid body dynamics of the model. However, since the windoff structural damping levels of the model and airplane vibration modes were similar, it is believed that structural damping differences did not contribute significantly to the differences in the model and airplane flutter speeds. The data shown in Fig. 9 indicate that the model and airplane have the same damping trends for the FMC system on condition, and that in both cases use of the FMC system increases the damping considerably at velocities near the open-loop flutter point. Although there are some differences in the measured damping values for the model and airplane, there is still good correlation between the two systems for similar FMC operating conditions. Thus, it can be concluded that the performance of the B-52 CCV airplane flutter suppression system was successfully simulated in the model tests.

Conclusions

A description of a flutter suppression study using a 1/30-scale aeroelastic model of the B-52 CCV airplane has been presented. The results show that the B-52 CCV active flutter suppression system was successfully simulated with the wind-tunnel model. They also indicate that the analysis used in the study was conservative in predicting the flutter velocity for both the model and airplane. The test data show that the model and airplane active control flutter suppression systems, which were based on phasing between wing motion and control-surface deflection, pro-

duced significant improvements in the damping of the flutter mode.

References

- ¹Wykes, J. H. and Kordes, E. E., "Analytical Design and Flight Tests of a Model Suppression System on the XB-70 Airplane," *Aeroelastic Effects From a Flight Mechanics Standpoint*, AGARD CP-46, 1970, pp. 23-1-23-18.
- ²Burris, P. M., Dempster, J. B., and Johannes, R. P., "Flight Testing Structural Performance of LAMS Flight Control System," AIAA Paper 68-244, Los Angeles, Calif., 1968.
- ³Arnold, J. I. and Thompson, G. O., "B-52 Controls Configured Vehicle System Design," AIAA Paper 72-869, Stanford, Calif., 1972.
- ⁴Stockdale, C. R. and Poyneer, R. D., "Control Configured Vehicle Ride Control System (CCV-RCS)," AFFDL-TR-73-83, July 1973, Air Force Flight Dynamics Lab., Wright-Patterson Air Force Base, Ohio.
- ⁵Bergmann, G. E. and Severt, F. D., "Design and Evaluation of Miniature Control Surface Actuation Systems for Aeroelastic Models," AIAA Paper 73-323, Williamsburg, Va., 1973.
- ⁶Abel, I. and Sandford, M. C., "Status of Two Studies on Active Control of Aeroelastic Response," TM X-2909, Sept. 1973, NASA.
- ⁷Boeing Document D3-7387-1, "Design Control Specifications for a One-Thirtieth Scale B-52E Flexible Model," USAF Contract F33615-67-C-1264, June 1967, The Boeing Company, Wichita, Div., Wichita, Kan.
- ⁸Gilman, J., Jr. and Bennett, R. M., "A Wind-Tunnel Technique for Measuring Frequency-Response Functions for Gust Load Analyses," *Journal of Aircraft*, Vol. 3, No. 6, Nov.-Dec. 1966, pp. 535-540.
- ⁹Boeing Document D3-9224, "Development of Active Flutter Suppression Wind Tunnel Testing Technology—Interim Report," USAF Contract F33615-73-C-1913, Sept. 1973, The Boeing Company, Wichita Div., Wichita, Kan.
- ¹⁰Hodges, E., "Active Flutter Suppression—B-52 Controls Configured Vehicle," AIAA Paper 73-322, Williamsburg, Va., 1973.
- ¹¹Reed, W. H., III and Abbott, F. T. Jr., "A New 'Free-Flight' Mount System for High-Speed Wind-Tunnel Flutter Models," *Proceedings of Symposium on Aeroelastic and Dynamic Modeling Technology*, RTD-TDR-63-4197, Pt. 1, March 1964, Systems Command, Dayton, Ohio, pp. 169-206.
- ¹²Keller, A. C., "Vector Component Techniques: A Modern Way to Measure Modes," *Sound and Vibration*, Vol. 3, No. 3, March 1969, pp. 13-26.
- ¹³Cole, H. A., Jr., "On-Line Failure Detection and Damping Measurement of Aerospace Structures by Random Decrement Signatures," CR-2205, 1973, NASA.